Reconstruction of the wave climate in the Proper Baltic Basin, April1947 – March1988

M. Mietus, H. von Storch

Abstract

The present paper characterizes the Empirical Orthogonal Functions of daily maximum values of the total significant wave height and corresponding wind waves and swell heights in the Proper Baltic Basin using a 5 year hindcast data set, April 1988–March1993. For this data set and particular seasons the empirical transfer functions between large-scale air-pressure and the mesoscale wave fields were computed by means of Canonical Correlation Analysis. In this semi-enclosed basin, computed canonical pairs show dependence of wave fields on the wind, the distance from the shore and on the bathymetry. Furthermore, air-pressure data for 42 years were used to reconstruct wave climate in the considered basin. The reconstructed time series show annual/seasonal and multi-annual/multi-seasonal variability. Statistically significant trends could not be detected for the reconstruction period.

Rekonstruktion des Wellenklimas in der zentralen Ostsee für den Zeitraum April 1947 bis März 1988

Zusammenfassung

In der vorliegenden Arbeit werden die Empirisch Orthogonalen Funktionen der täglichen Maxima der signifikanten Wellenhöhe sowie der in ihr enthaltenen Windsee und Dünung in der zentralen Ostsee beschrieben. Als Datengrundlage dienen reanalysierte Beobachtungen aus dem Zeitraum April 1988 bis März 1993. Für verschiedene Saisons werden mittels Kanonischer Korrelationsanalyse statistische Modelle zwischen dem großskaligen Luftdruckfeld und dem mesoskaligen Wellenfeld angepaßt. Die erhaltenen Muster zeigen die Abhängigkeit des Wellenfeldes vom Wind, der Küstennähe und der Wassertiefe. Das großskalige Luftdruckfeld und die statistischen Modelle werden dann benutzt, um das Wellenklima in der zentralen Ostsee für den Zeitraum April 1947 bis März 1988 zu rekonstruieren. Die rekonstruierten Daten zeigen Variabilität auf saisonaler, jährlicher und niederfrequenterer Skala. Statistisch signifikante Trends treten in den rekonstruierten Daten nicht auf.

1 INTRODUCTION

When long-term observation al time series are lacking, statistical methods can be useful to reconstruct past variability and to detect existing trends. Of special interest are downscaling techniques, with which one can find the empirical transfer function between large-scale fields of independent data and the mesoscale fields. These dependent data are often called local data in climate research. The condition for application of downscaling is the existence of long homogeneous time series, which are indispensible for the fit and confirmation of the statistical relationship.

In the present paper the sea level air-pressure is taken as the large-scale parameter and the daily maximum of the total significant waves height and corresponding wind wave and swell height are taken as local parameters.

In Section 2 the Empirical Orthogonal Functions method is described, and data sets and computed patterns are presented. Section 3 deals with Canonical Correlation Analysis and shows the empirical transfer functions between large-scale air-pressure field and wave fields in the Proper Baltic Basin. In Section 4 the results of reconstructed wave climate are discussed. In Section 5 a brief summary is presented.

2 EMPIRICAL ORTHOGONAL FUNCTIONS OF THE PROPER BALTIC WAVE FIELDSANDLARGE-SCALE SEALEVELPRESSURE

2.1METHOD

When analyzing climate data sets the full phase space is often split into two subspaces. The main space, called the "signal" subspace, is described by some few time independent characteristic patterns. The "signal" subspace represents the dynamics of considered process. The second subspace called the "noise" subspace, is high-dimensional and includes all processes irrelevant for the "signal" subspace. The problem is to properly separate "signal" and "noise". According to von Storch (1995), in climate research the signal is defined by the interest of the researcher and the noise is everything else unrelated to this object of interest. One of the techniques applied to identify patterns of simultaneous variations is the well-known

method of Empirical Orthogonal Functions. Decomposition of the full phase space into a "signal" subspace can be formally written as

$$\vec{X}(t) = \sum_{k=1}^{M} (\alpha_k(t) \cdot \vec{e}_k(t)) + \vec{n}(t)$$

where time coefficients alt) describe the dynamics of the "signal" subspace and $\bar{e}_k$ are the fixed patterns. The number M is usually much smaller than the dimension of $\overline{X}(t)$. The patterns are chosen to be orthogonal. In the result, time coefficients $\alpha_k(t)$ are obtained by projection of $\overline{X}(t)$ onto the patterns $\bar{e}_k$. The αj are normalized to Var(αj)=1 so that the patterns carry the "typical" magnitude. Additionally the expansion coefficients $\alpha_k(t)$ must minimize the error

$$\varepsilon(\vec{\alpha}) = \langle \vec{X}(t) - \sum_k (\alpha_k(t) \cdot \vec{e}_k(t)) | \vec{X}(t) - \sum_k (\alpha_k(t) \cdot \vec{e}_k(t)) \rangle$$

where $< \bar{a} | \bar{b} > = \Sigma_j a_j b_j$ denotes "dot product". Patterns defined as above are called *Empirical Orthogonal Functions* (EOFs), and the corresponding time series are called the *EOF's coefficients or the Principal Components (PCs)*.

An adequate measure to quantify the relative importance of one pattern or a set of patterns is the amount of explained variance η defined as

$$\eta = 1 - Var\left(\vec{X}(t) - \sum_k \alpha_k(t) \cdot \vec{e}_k\right) / Var(\vec{X}(t)) = \left(\frac{1}{N}\right) \sum_{j=1}^{N} \eta(\vec{X}_j(t))$$

2.2 EMPIRICAL ORTHOGONAL FUNCTIONS OF THE PROPER BALTIC WAVE FIELDS

To derive EOFs for the Proper Baltic wave fields, the integrated characteristics of wave field were used. These characteristics come from a 5-year hindcast from April 1988 to March 1993.

They were derived using the shallow water version of the HYPA (Hybrid PArametrical Water Wave Model, Guenther et al., 1979,1981,1984) used by the GKSS Research Center in Geesthacht to characterize the wave climate in the Baltic Sea (Gayer, Guenther, Winkel, 1995). Integrated parameters of model output have a 3-hour time step and about 16 km resolution in space. For every day, the wave field with maximum of total significant wave height were determind for 3 different grid point sets (Fig.l) and decomposed into a wind wave and swell contribution. For these contribution, the wind wave and swell height were derived. For the first data set (N_a) only 58 uniformly distributed grid points were used, for the second set (N_b), 118 points, and for the fine mesh data set (N_c) as many as 231 grid points. In the latter case nearly 25% of model grid points were used, while for a coarse network just 7% were used. Using these three networks for each calendar month EOFs, were computed for the daily data. Additionally explained variances were also calculated. Computed values for total significant wave height are presented in Table 1.

Table 1: Amount of variance (in per cent) of total significant wave height explained by the three first EOFs in particular networks

Month	1st EOF	1st EOF	1st EOF	2nd EOF	2nd EOF	2nd EOF	3rd EOF	3rd EOF	3rd EOF
	N_a	N_b	N_c	N_a	N_b	N_c	N_a	N_b	N_c
Jan.	85	85	85	8	9	9	2	4	4
Feb.	81	81	81	9	9	9	4	6	6
Mar.	83	84	84	9	9	9	4	6	6
Apr.	68	68	68	16	18	18	6	6	6
May	67	70	70	17	15	15	6	7	7
Jun.	71	71	71	12	14	14	7	8	8
Jul.	74	74	74	10	11	11	7	8	8
Aug.	71	70	70	13	14	14	7	7	7
Sep.	83	83	83	8	9	9	3	4	4
Oct.	83	83	83	7	8	8	4	6	6
Nov.	76	77	77	12	13	13	4	6	6
Dec.	81	81	81	9	9	9	3	5	5

There are two dinstinct seasons characterized by different distributions of variance between

particular patterns. The first, which might be called "cold" or "stormy", includes the months from January to March and from September to December. The second, called "warm" or "ca1m", spans the period from April to August. The names "stormy" and "ca1m" seasons better describe the climatic features of the region, since from September to March the Baltic Sea Basin is influenced by the zonal circulation of a relatively high-pressure gradient. Mean monthly wind speed in the "stormy" season varies between 14 and 18 knots over the sea, and the percentage of observations with strong breeze (wind speed 11 ms¹) ranges from 10-20% at the coasts to 30-40% in the central part of the Proper Baltic. Minimum wind speeds are observed in the "ca1m" months, with the highest number of such cases in August. In summer the percentage of observations of strong breeze ranges from 5% on the coasts to near 10% on the open sea (Mietus, Wielbinska, 1996, Mietus, Kaufeld, Heino, 1997). Table 1 also shows that the amount of variance explained by the EOFs for each month and each network type does not depend on the spatial resolution of the networks. In spite of a significant increase in resolution, no significant changes in the amount of explained variance could be found.

Table 2: Amount of variance (in per cent) explained by successive EOFs for the heights of total significant wave (T), wind wave (W) and swell (S) in the Proper Baltic Sea

Resolution type N_a

	T	T	T	W	W	W	S	S	S
Season	1stEOF	2ndEOF	3rdEOF	1stEOF	2ndEOF	3rdEOF	1stEOF	2ndEOF	3rdEOF
Calm	71	13	7	71	13	6	56	12	10
Stormy	83	8	3	83	8	3	57	14	9
Year*	83	8	3	83	8	3	59	13	9

Resolution type N_c

Season	1stEOF	2ndEOF	3rdEOF	1stEOF	2ndEOF	3rdEOF	1stEOF	2ndEOF	3rdEOF
Calm	71	13	6	71	13	6	56	13	9
Stormy	83	9	3	82	8	3	58	13	9
Year*	82	8	6	82	8	3	60	12	9

* Year stands for the time April 1988-March 1993

This conclusion is not only important, but also very practical as it allows one to spare

computing time. The variance explained by particular patterns was recalculated separately for the "stormy" and the "ca1m" seasons and for the whole year. Computations were made for each component of the wave field.

Results are presented in Table 2 for coarse (N_a) and fine (N_c) networks. These computations confirm the earlier results concerning selection of optimum grid points network. This information is of great value for the construction of empirical transfer functions between large-scale air-pressure field and components of mesoscale wave fields, discussed in the following sections.

The amount of variance explained by particular patterns illustrates the relative strength of the patterns in question. In case of the "year" and the "stormy" season the first three EOFs explain more than 94% of variance, both for total significant wave height and for wind wave height. This fact, together with significant similarities between corresponding modes (Fig.2), show that the process of wave generation in the Proper Baltic Basin has a relatively large-space scale and that wind plays the dominant role. The first patterns (Fig.2), for both total wave fields, reveal a significant anomaly of wave height in almost the entire region. Such patterns can be easy explained by the domination of southwesterly and westerly winds in the region and by the effect of its fetch on the waters off the western and southern coasts. The second patterns (Fig.2) describe an opposite anomaly of waves heights (so-called "see-saw") along the main axis of the basin, oriented from the southwest to the northeast. The zero-anomaly isoline crosses the Proper Baltic Sea Basin south of Gotland from the Swedish to the Latvian coast. The third patterns (Fig.2) present similar oscillation between the western and the eastern parts of the basin. The zero isoline in this case runs from the central part of the Archipelago Sea in the north to the central Polish coast in the south. In spite of some differences between corresponding patterns for the total and wind wave fields as well as between those generated for the coarse and the fine grid networks, these discrepancies are not important and do not modify the main features described above. For the "calm" season, the first three patterns explain about 90% of variance. The similarities between corresponding patterns for a total and wind wave fields are stronger than during the "stormy" season. There are still small differences between patterns for the fine and the coarse networks. It should be pointed out that there are also good similarities between patterns generated for the "calm" and the "stormy" season.

For swell, the amount of variance explained by the first EOFs in particular seasons differs

somewhat. However, the first patterns (Fig.3) are rather similar to each other and show maximum of anomaly in the central part of the Proper Baltic, between Gotland and the eastern coast. The second patterns (Fig.3), both for the "year" and the "stormy" season, describe an opposite distribution of swell anomaly between the northern and the southeastern parts of the basin. The zero isoline crosses the basin from Rugia in the south to the south of Saremaa at the entrance to the Gulf of Riga. The third patterns (Fig.3) describe "see-saws" between the western and eastern coasts and the zero isoline extends from the Aland Sea to the Cape of Rozewie.

The patterns of swell for the "ca1m" season a represented on Figure4.

There are significant similarities between corresponding patterns for the total and wind waves in case of either season. In spite of some differences showed in Figures 3 and 4 it should be noted that there are also strong similarities between patterns for the swell in case of each considered seasons. The factor which allows one to distinguish between corresponding patterns is the maximum amplitude of the anomaly. While for the "stormy" season the anomalies of the first EOFs reach 1.4m both for the total and the wind wave, for the "year" they reach 1.2m and for the "ca1m" season they are only about of 0.8m (Table 3). The similar relationship occurs also for the second EOFs. Much smaller anomalies are characteristic for swell.

Table3: Extreme values of anomalies (in meters) of particular EOFs for the total wave (T), wind wave (W) and swell (S) in the Proper Baltic Sea

Season	T/W	T/W	T/W	S	S	S
	1stEOF	2ndEOF	3rdEOF	1stEOF	2ndEOF	3rdEOF
Stormy	-1.40	+0.60 (N) -0.40 (S)	+0.20 (E) -0.20 (W)	-0.40	+0.25(N) -0.20 (SE)	+0.10 (E) -0.15 (W)
Calm	-0.80	+0.40 (N) -0.40 (S)	+0.20 (E) -0.20 (W)	-0.30	+0.15 (N) -0.10 (S)	+0.10 (W) -0.10 (SE)
Year*	-1.20	+0.50 (N) -0.40 (S)	+0.20 (E) -0.20 (W)	-0.35	+0.20 (N) -0.15 (S)	+0.10 (E) -0.15 (W)

* *Year stands for the time April 1988-March 1993. The letters in brackets denote the region of the basin in which maximum of anomaly occurs*

2.3 EMPIRICAL ORTHOGONAL FUNCTIONS OF LARGE-SCALE AIR-PRESSURE

To compute the large-scale sea level air-pressure patterns the NCAR data set (the National Center for Atmospheric Research) of daily mean values of sea level air-pressure was used. The daily mean values were computed based on data from 00 and 12 UTC, at a 5°x5° spatial resolution in the area bounded by 75°N, 35°N, and 50° Wand 40°E. Since the hindcast data cover the years April 1988 -March 1993, the computed patterns cover this same period. According to Trenberth and Paolino (1980) we can assume that air-pressure data are homogenous.

When the data for the whole year are considered, the first pattern presents a large pressure system covering nearly the entire region (Fig.5). The center of this system is located west of Scotland. This pattern explains 27% of the variance. The second mode (Fig.5), explaining 20% of variance, shows a large system with its center over The Netherlands. The Baltic Sea is under the influence of this pressure system while the northwestern and northern part of the region is covered by a system of opposite sign. The third pattern (Fig.5) explains 15% of variance, and shows two large centers. The continental, eastern part of the region is under the influence of a large system while the western part is dominated by a pressure system of opposite sign. The fourth pattern (Fig.5) explains 7% of the variance. It presents two centers of the same sign located over the southwestern and the northeastern parts of the region. The central part is covered by pressure system of opposite sign. The southwestern Baltic Sea is on the edge of this system while the rest of the basin is under the influence of the northeastern center. The fifth pattern explains 6%, the sixth, 5%, and the others, each less than 4% of variance. The cumulative variance for patterns one to four is greater or equal to 80% for the Baltic Sea Basin. Therefore, any patterns of order higher than four can be neglected.

The "stormy" season modes are similar to those for the annual case, with some differences of course. They explain, respectively, 28, 20, 16 and 7% of variance. Also in this case the cumulative variance exceeds 80% in the region of interest.

Figure 6 presents the first four EOFs for the "calm" season which explain 31,22, 13 and 7% of variance, respectively.

3 EMPIRICAL TRANSFER FUNCTIONS BETWEEN LARGE-SCALE AIR-PRESSURE FIELD AND MESOSCALE WAVE FIELDS IN THE BALTIC SEA BASIN

3.1 METHOD

The canonical correlation analysis (CCA) is a good tool for the estimation of empirical transfer functions between large-scale sea level air-pressure field and the components of mesoscale wave fields. The CCA expands two simultaneously observed fields P and H into

$$P(x, t) = \sum_{i=1}^{M} S_i(x) \cdot u_i(t)$$

$$H(x', t) = \sum_{j=1}^{N} G_j(x') \cdot v_j(t)$$

where $S_i(x)$ and $G_i x'$) and are the *i-th* "CCA-patterns" and u_i, v_i are the *i-th* "*canonical time series*". The canonical time series are orthogonal in the sense that they fulfill the following conditions

$$\langle \vec{u}_i(t) | \vec{u}_j(t) \rangle = \langle \vec{v}_i(t) | \vec{v}_j(t) \rangle = \delta_{ij}$$

$$\langle \vec{u}_i(t) | \vec{v}_j(t) \rangle = \delta_{ij} \cdot r_i$$

where r_i describes the correlation between the pair of time series. The time series u_l and v_l have   a maximum possible correlation, u_2 and v_2 have the next highest correlation by being   orthogonal to the former pair, and so on. The *canonical patterns (canonical maps)* are vectors whose components show the correlation at specific locations (x or x') between P and H and their respective canonical time series. The detailed description of the CCA method can be found in Barnett and Preisendorfer (1987).

3.2 EMPIRICAL TRANSFER FUNCTIONS

To calculate the correlation between large-scale sea level air-pressure and wave fields in the Proper Baltic Sea, the data sets mentioned above were used. The computations were performed for the time April 1988 - March 1993, as above.

To ensure that the correlations are not dominated by common linear trends, they were subtracted from both time series. The same was done with the annual and semi-annual cycles.

To construct the empirical transfer functions, the first four patterns for pressure and the first three patterns for each of the wave field components were used for the "year" and the "stormy" season. The number of sea level pressure modes was increased to five for the "ca1m" season. As only three wave modes were used each time, only three pairs of empirical transfer functions were obtained in each case.

For the "year", the first pair of canonical maps (Fig.7) shows a large-scale negative air-pressure anomaly over the nearly whole considered region, with maximum of about 10 hPa over southern Scandinavia. Because of this, the Proper Baltic Sea region is located in the west wind zone. This pattern explains 27% of air-pressure variance. Its time series is linked with a correlation coefficient of 0.55 to the time series of the total waves pattern, which describes a simultaneous increase of total waves in the entire Proper Baltic Basin. This increase intensifies with increasing distance from the western coast. This wave pattern explains as much as 85% of the total waves variance. The second pair (Fig.7) describes the pressure anomaly over the Atlantic Ocean and the western part of the European continent with the center of about10 hPa located northwest of Ireland. The western part of the Proper Baltic is on the edge of this system, while the eastern part is on the edge of an opposite sign anomaly with its center over Russia. This pattern explains 19% of pressure variance. The corresponding total wave pattern shows anomalies of opposite sign in the northern and the southern part of the Proper Baltic. This pattern explains 7% of total wave variance, with a correlation coefficient between corresponding time series of 0.37. The third canonical pair (Fig.7) presents a NAO-like pattern for the pressure (a greater part of the Baltic Sea including the Proper Baltic is under the influence of a low while the Gulf of Bothnia is under the influence of a high). This pair reveals also the opposite anomaly of waves height which of isolines lying perpendicular to the main axis of the basin. The third patterns explain 13% of air-pressure variance and 6% of total wave height variance. The correlation coefficient is 0.26. There are significant similarities between

corresponding patterns for the total and the wind waves. The amounts of explained variance are nearly the same. There are no differences in case of corresponding correlation coefficients.

In case of the "stormy" season the empirical transfer functions between air-pressure and total waves or wind waves are identical (Fig.8).

For the "calm" season the similarities between the empirical transfer functions computed for total waves and wind waves are as in previous cases very high. Therefore, only canonical pairs for air-pressure and total waves are presented on Figure 9.

The empirical transfer functions between air-pressure and swell were computed for different values of time lag between pressure and swell data. Due to fact that a swell could be called "memory of the former sea state" and taking into account that estimated time for the swell to cross the Baltic Sea from north to south is about 26-30 hours (personal communication with H. Guenter, GKSS), the computations were proceeded for lags of 0,1 and 2 days. In each case (for each season) no changes in correlation between the corresponding time series have been found. It should be pointed out that no significant differences between computed empirical transfer functions could been seen. It means that there is only a very weak physical link between air-pressure and the swell field in the Proper Baltic Basin. Therefore, only one set of canonical pairs, for the "calm" season is presented here (Fig.l0).

4 RECONSTRUCTION OF THE WAVE FIELDS IN THE PROPER BALTIC BASIN

4.1 METHOD

To reconstruct wave fields anomalies from the large scale air-pressure data the strategy described by von Storch et al. (1993), Cui et al. (1995) or Heyen et al. (1996) was implemented. Let P' and H' be independent data which are assumed to share respectively the same canonical maps as P and H. Therefore we could write sub-signal P' in the form as follow

$$P'(x, t) = \sum_{i=1}^{m<M} S_i(x) \cdot u'_i(t) + \varepsilon$$

where the error ε is minimized by the least square method and a new time series $u'i(t)$ is

calculated. Supposing that $u'_i(t)$ is correlated with $v'_i(t)$ in the same manner as $u'_i(t)$ and $v'_i(t)$ it is possible to estimate $v'_i(t)$ as $v'_i(t) = r_i\, u'_i(t)$. Finally neglecting the error ε it could be written that

$$H'(x', t) \approx \sum_{j=1}^{n \leq N} H_j(x') \cdot v'_j(t) = \sum_{j=1}^{n \leq N} H_j(x') \cdot u'_j(t) \cdot r_j$$

where the reduced number of retained patterns and time series is marked by n.

4.2 RESULTS OF RECONSTRUCTION

To reconstruct wave fields in the Baltic Sea Basin by means of empirical transfer functions between a large scale air-pressure field and the wave fields, the NCAR data set was once again used. This time pressure data from April 1947 - March 1988 were selected as independent data. For the purposes of reconstruction, the independent data were allowed to contain linear trends. By means of formula (9), as above, the fields of total waves, wind waves and swell were reconstructed for the "year" as well as for the "stormy" and the "calm" seasons. Because the swell is rather short in the Baltic Sea the total wave does not differ much from the wind wave. Therefore, only the total wave reconstruction for the points A-D in Figure 1 are presented (Figs 11-12). Points A and C are located near the coast, A near the German coast and C near the southern cape of Gotland. The water is shallow at both points and both are in the aerodynamic shadow of the adjacent land, so the reconstructed series show variations of the amplitude anomaly between -1.2m and 1.2 m. At point B (30 km east of Hel in the Gulf of Gdansk) the amplitude of anomaly of the reconstructed time series varies between -1.6m and +1.6m. This could be explained by the effect of deep water and of the wind fetch, which is here greater than at points A and C. The changes of amplitude in range of 3m can be recognized in case of point D, in the open sea, in deep water, far from the coast. For none of the reconstructed time series could any statistically significant trends be detected. However, some groups of seasons/years with increasing or decreasing tendencies of wave height could be found. Additionally, the reconstructed time series show seasonal (annual) and multi-seasonal (multi-annual) variations.

5 SUMMARY

There are two distinct seasons, with different characteristics, of the wave climate over the Proper Baltic Sea Basin. In the "stormy" season, from September to March, the first Empirical Orthogonal Functions explain more than 80% of variance of the total waves for each month. In the "calm" season, from April to August, the variance explained by the first pattern is greater than 67% for each month. The amount of variance explained by the first three modes for the whole year and both seasons is greater than 90% for the total and the wind waves, and is nearly 80% for swell. Computations conducted for the three kinds of grid network show that the amount of variance explained by particular patterns does not depend on an increasing number of grid points. This means that the wave generation process quickly covers the entire basin. The particular modes of total and wind waves are significantly similar and describe: (1) a simultaneous increase of wave height over the whole basin which is much higher in the central part of the open sea, (2) an opposite anomaly of wave height between the northern and the southern parts of the basin as well as between the western and the eastern parts of the basin. Canonical Correlation Analysis reveals a strong connection between the large-scale sea level air-pressure and the total and wind waves fields in any season. The generated canonical pairs confirm that the wind speed and direction, the distance from the coast, the fetch of the wind, and the bathymetry all playa significant role in generating wave fields in this small and semi-enclosed basin. The connection between air-pressure field and swell in this basin is much weaker and the relations of time shift between the force (pressure) and the swell could not be found by means of the computing techniques applied. The air-pressure canonical maps correlated with the first wave patterns describe the pressure anomalies with centers over the Baltic Sea and its vicinity. In case of the total and the wind waves these pressure anomalies are significant. The constructed empirical transfer functions are very useful for the reconstruction of past wave climate. The reconstructed time series reflect the local properties of the area, such fetch, aerodynamic shadow of the coast, and bathymetry. The variation of reconstructed series describes annual/seasonal and multi-annual/multi-seasonal periodicity and does not show any statistically significant trends.

ACKNOWLEDGMENTS

REFERENCES

Barnett, T. and Preisendorfer, R. 1987. Origins and levels of monthly and seasonal forecast skills for United States surface temperatures determined by canonical correlation analysis. *Mon. Wea. Rev.* **15**, 1825-1850.

Cui, M., von Storch, H. and Zorita E. 1995. Coastal sea level and the large scale climate state: a downscaling exercise for the Japanese Islands. *Tellus* **47A**, 132-144.

Gayer, G., Guenter H., Winkel N., 1995. Wave climatology and extreme value analysis for the Baltic Sea area off the Warnemuende harbour entrance. *Dt. Hydrogr. Z.* **47**, 2, 109-130.

Guenter, H., Rosenthai, W., Weare, TJ., Worthington, B.A., Hasselmann, K. And Ewing, J.A. 1979. A hybrid parametrical wave prediction model. *J. Geophys. Res.* **84**,5727-5738.

Guenter, H., Rosenthal, W., Dunckel M. 1981. The response of surface gravity waves to changing wind directions. *J. Phys. Oceanogr.* **11**,718-728.

Guenter, H., Komen, GJ., Rosenthal, W. 1984. A semi-operational comparison of two parametrical wave prediction models, *Dt. Hydrogr. Z.* **37**,89-106.

Heyen, H., Zorita, E., von Storch, H. 1996. Statistical downscaling of monthly mean North Atlantic air-pressure to sea level anomalies in the Baltic Sea, *Tellus* **48A**, 312-323.

Mietus. M., Wielbinska, D. 1996. Mean sea level pressure pattern over Europe and their local modifications over the Baltic Sea Basin, *Wiadomosci IMGW (Newsfrom IMWM)* **XIX**, z.3, 85-100 *(in Polish)*.

Mietus, M., Kaufeld, L., Heino, R. (eds.) 1997. Climate of the Baltic Sea Basin -final report of the WMO Project, *(submitted to WMO)*.

Trenberth, K.E. and Paolino jr.), D.A. 1980. The northern hemisphere SLP-dataset: trends,

errors and discontinuities. *Mon. Wea. Rev.* **108**, 855-872.

von Storch H., Zorita, E., Cubasch, U. 1993. Downscaling of global climate change estimates to regional scale: an application to Iberian rainfall in Wintertime. *J. Climate* **6**, 1161-1171.

von Storch H. 1995. Spatial Patterns: EOF's and CCA. *In: H.Von Storch and A.Navarra (eds.)* "*Analysis of Climate Variability: Applications of Statistical Techniques*", Springer, 1995, 227-258.
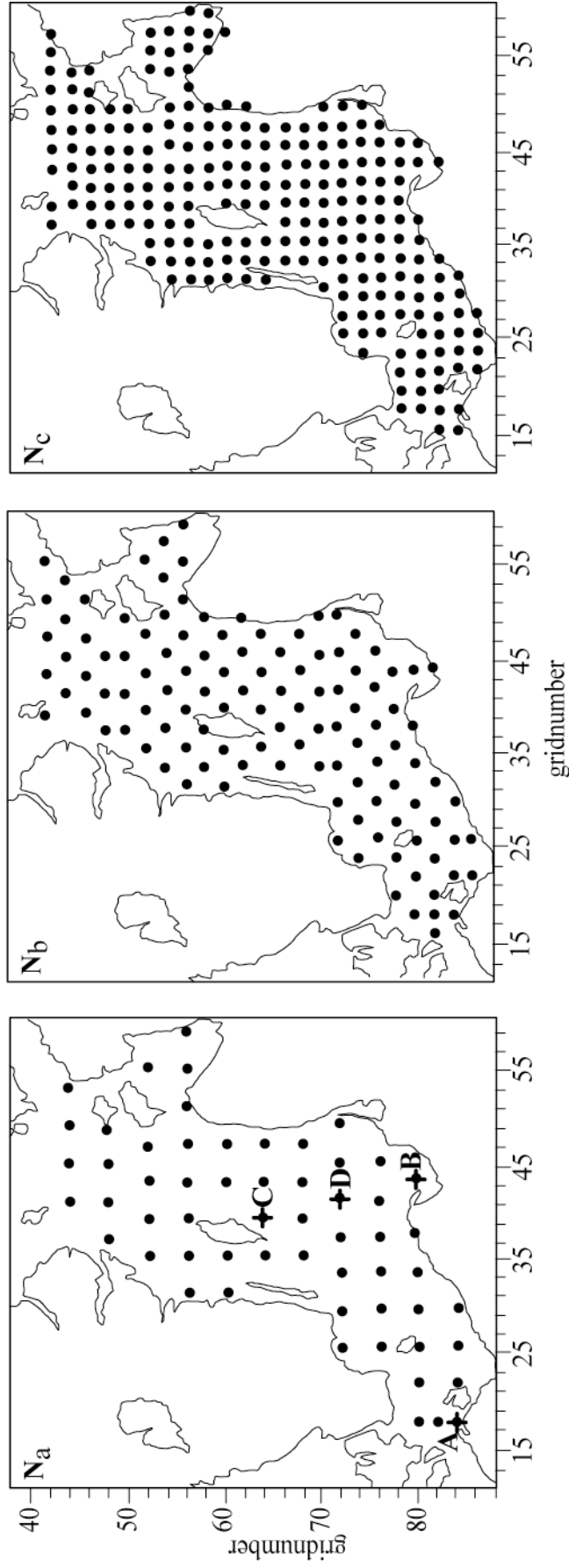
Fig. 1. Types of grid points networks used for estimate of EOFs. Points A to D, for which reconstructed time series are presented in Figs. 11–12, are marked by crosses.

20
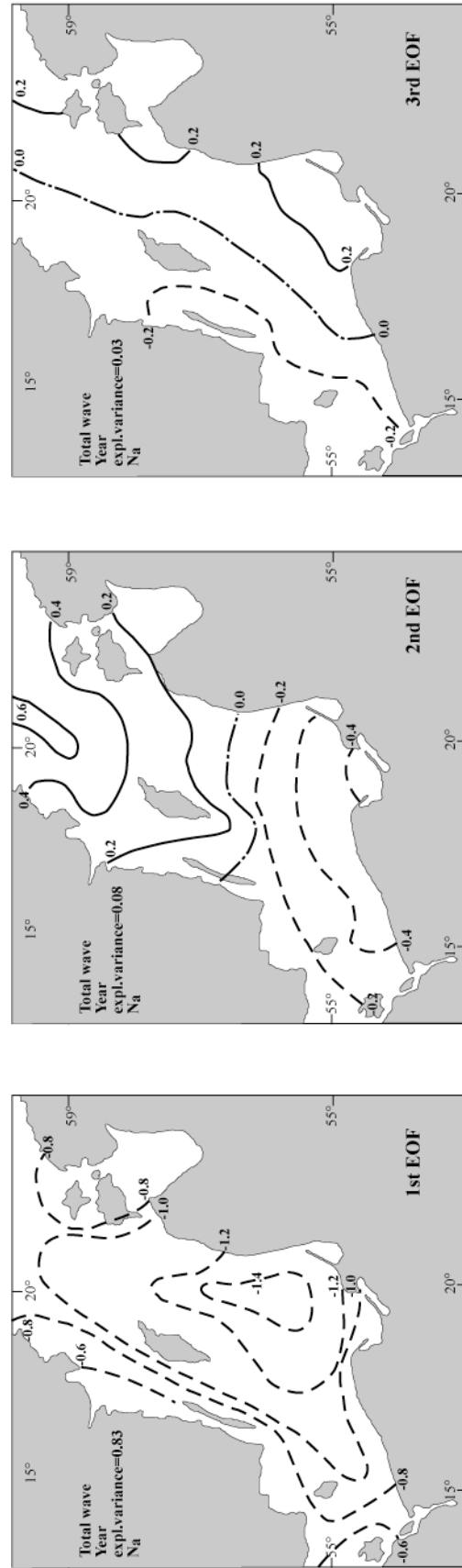
Fig. 2. The leading three patterns of total wave height anomaly for the whole year. Computations were based on daily maximum values of 8 values per day, from the time April 1988 - March 1993. Coarse network of grid (Na) was applied.
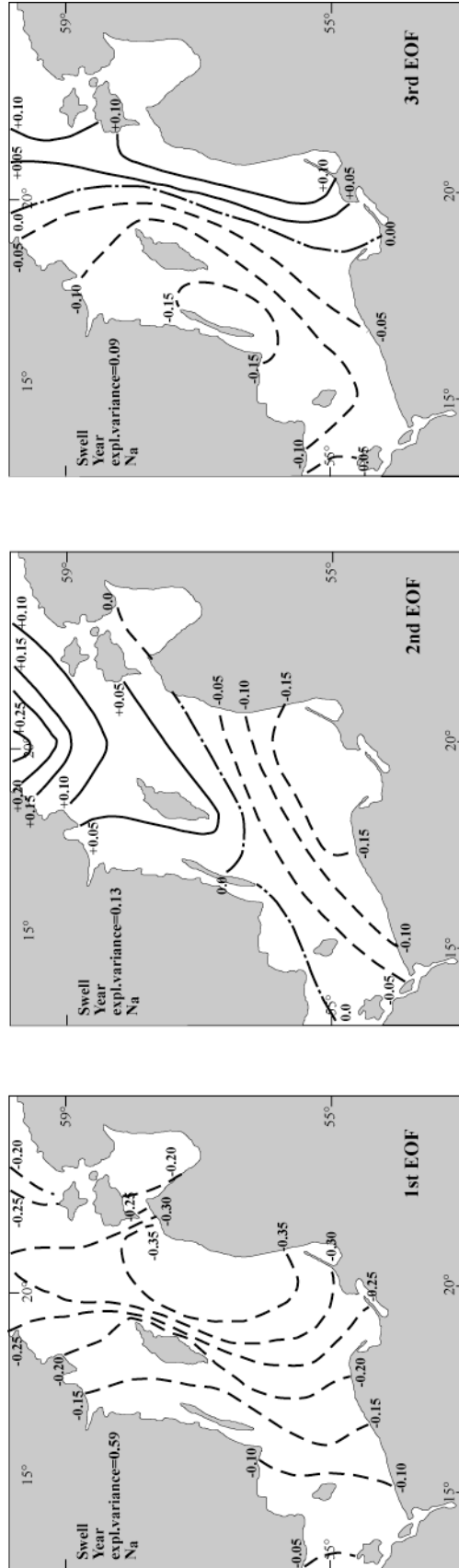
Fig. 3. The leading three patterns of swell for the year.
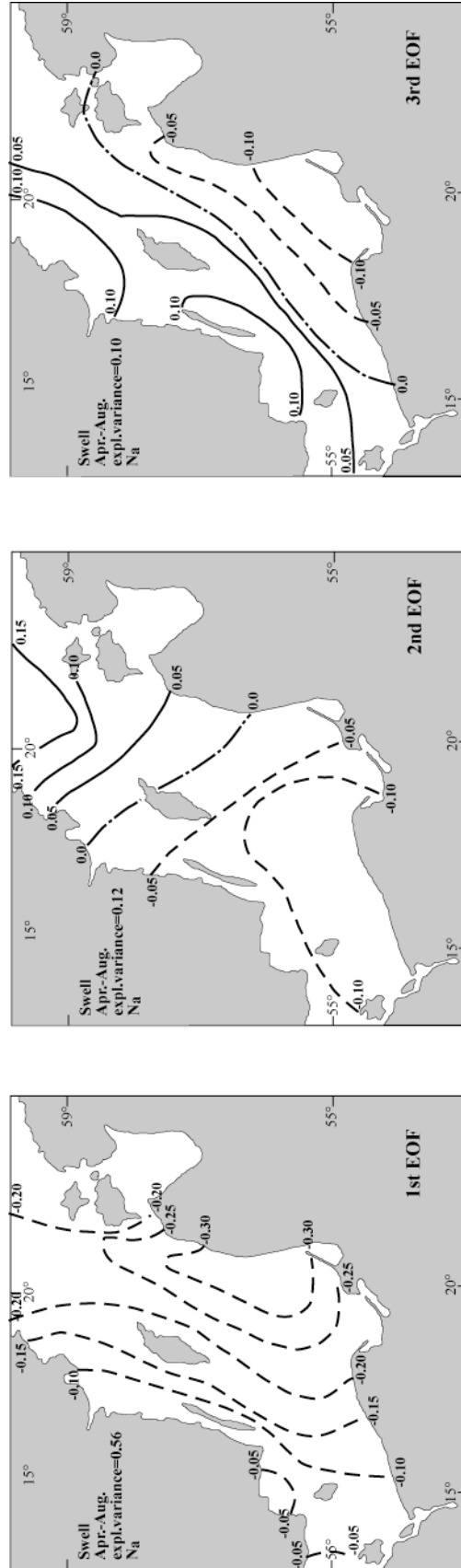
Fig. 4. The leading three patterns of swell for the "calm" season.
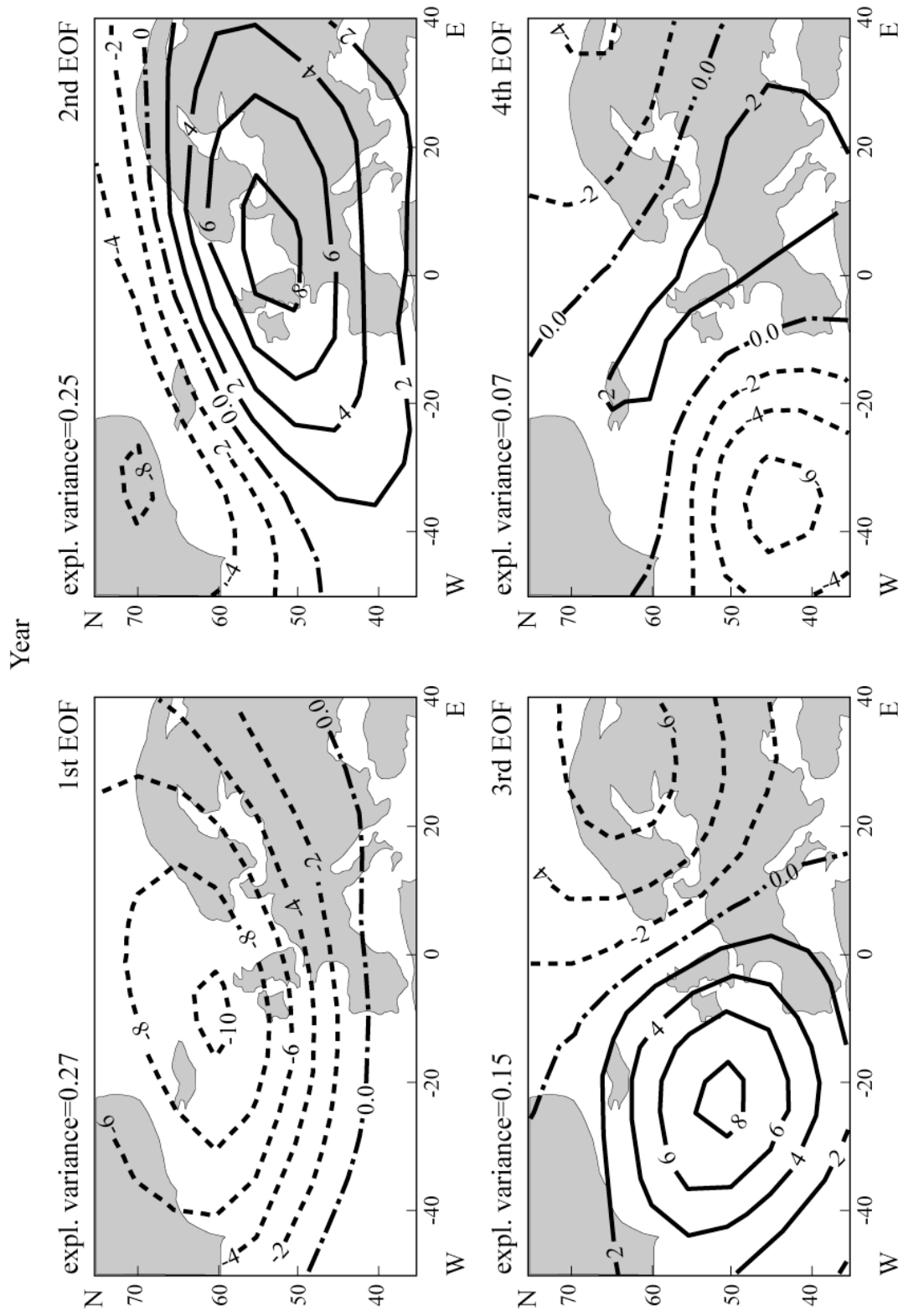
Fig.5. The first for EOFs of air pressure for the whole year. Computation were based on NCAR data set of daily mean values, at 5° x 5° resolution. Time: April 1988 - March 1993.
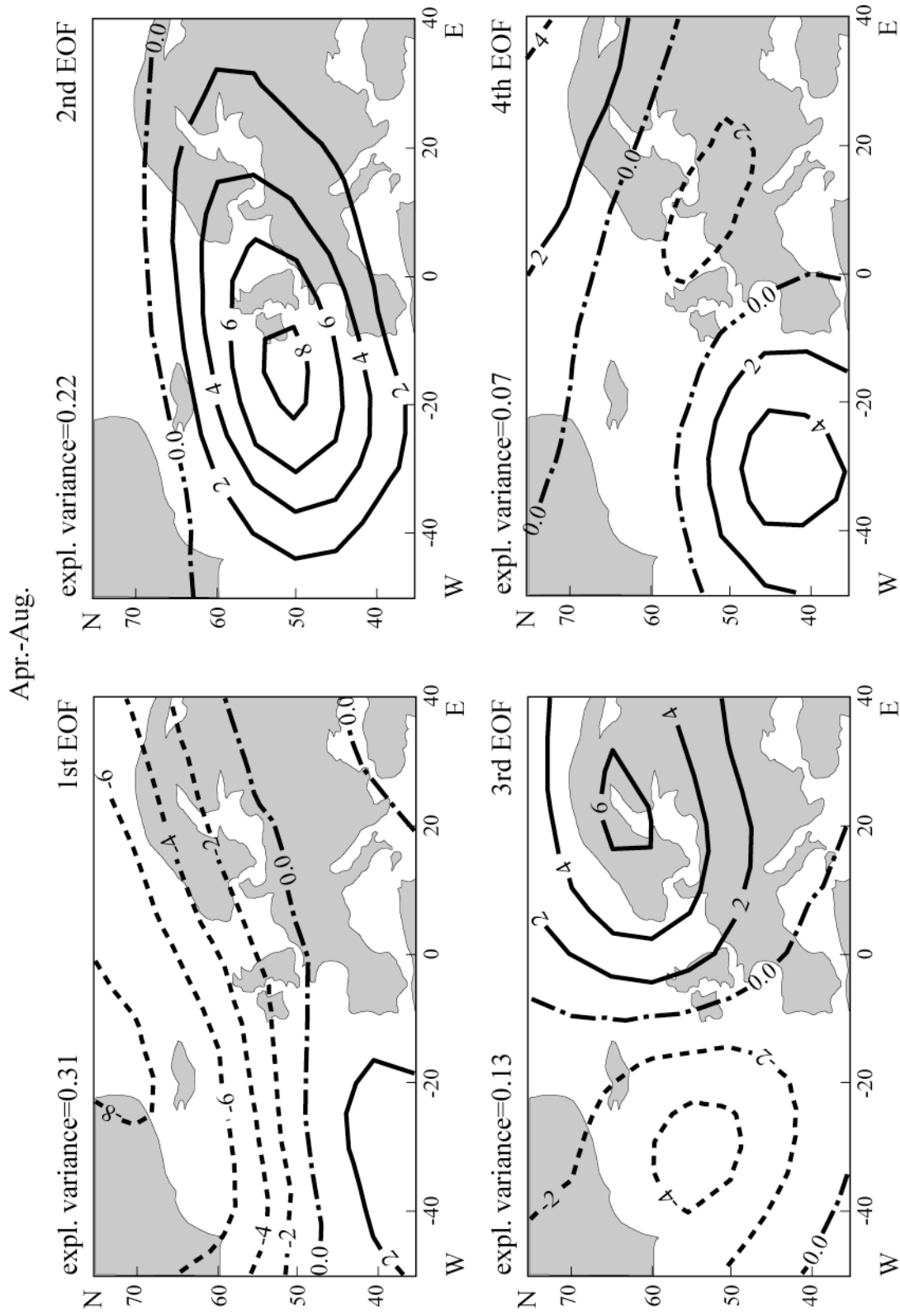
Fig.6. The first for EOFs of air pressure for the "calm" season.
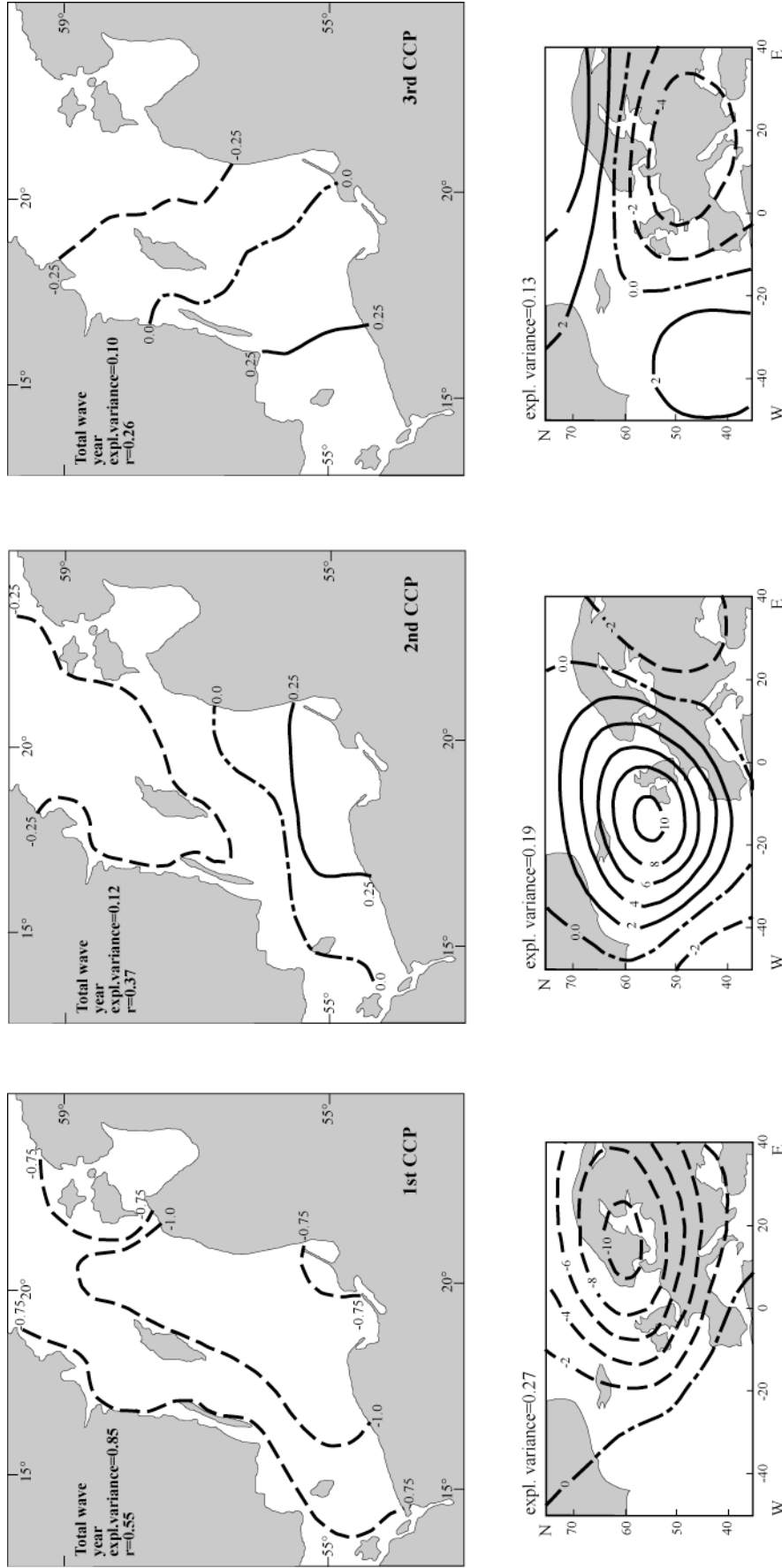
Fig. 7. Empirical transfer functions between largescale pressure fields and mesoscale wave fields on the Baltic sea. The three first CCA pairs (from left to right) of air pressure anomalies (hPa) and total wave height anomalies (m), for the whole year.
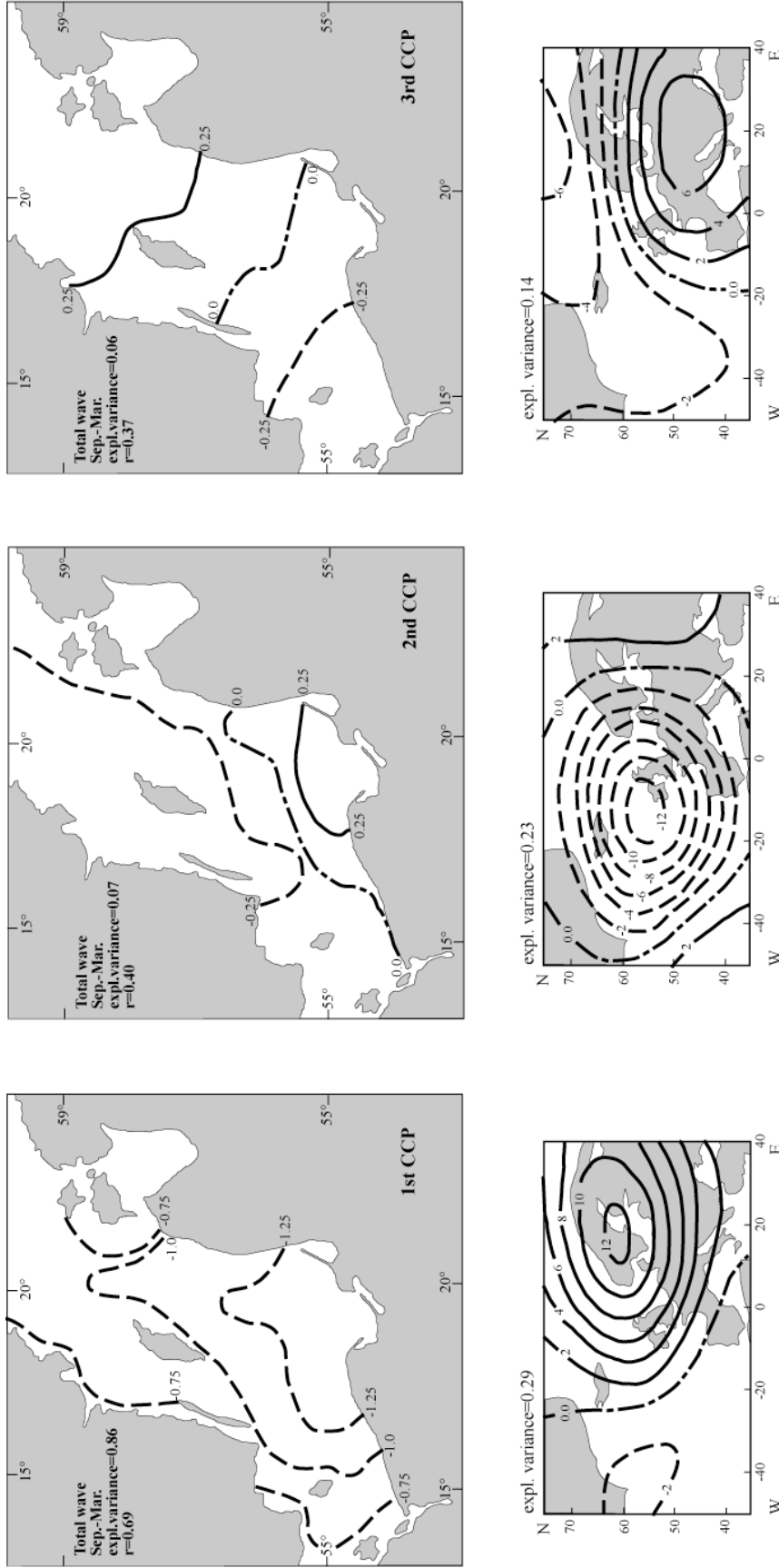
Fig. 8. The three first CCA pairs (from left to right) of air pressure anomalies (hPa) and total wave height anomalies (m), for the "stormy" season.
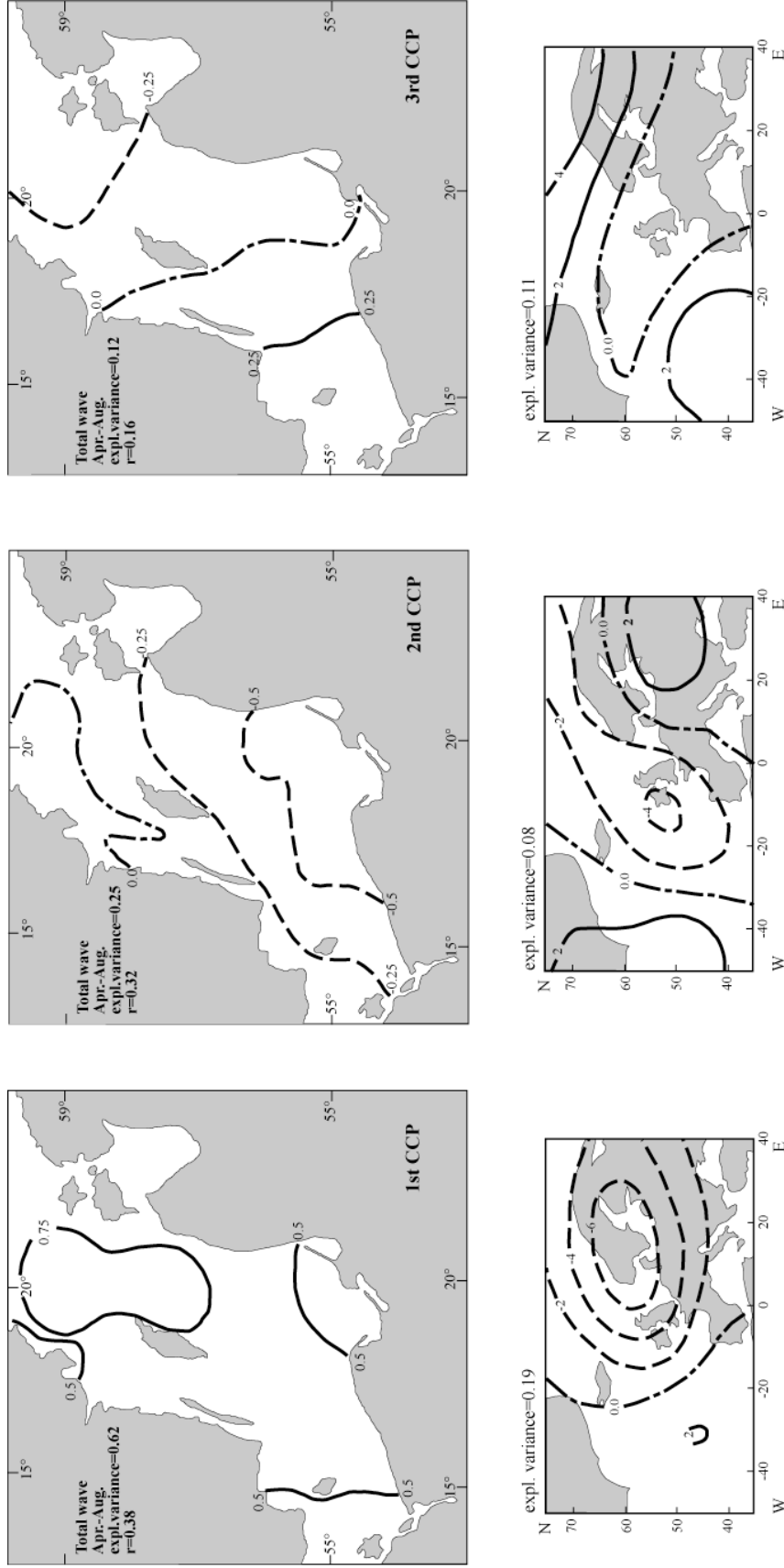
Fig. 9. The three first CCA pairs (from left to right) of air pressure anomalies (hPa) and total wave height anomalies (m), for the "calm" season.
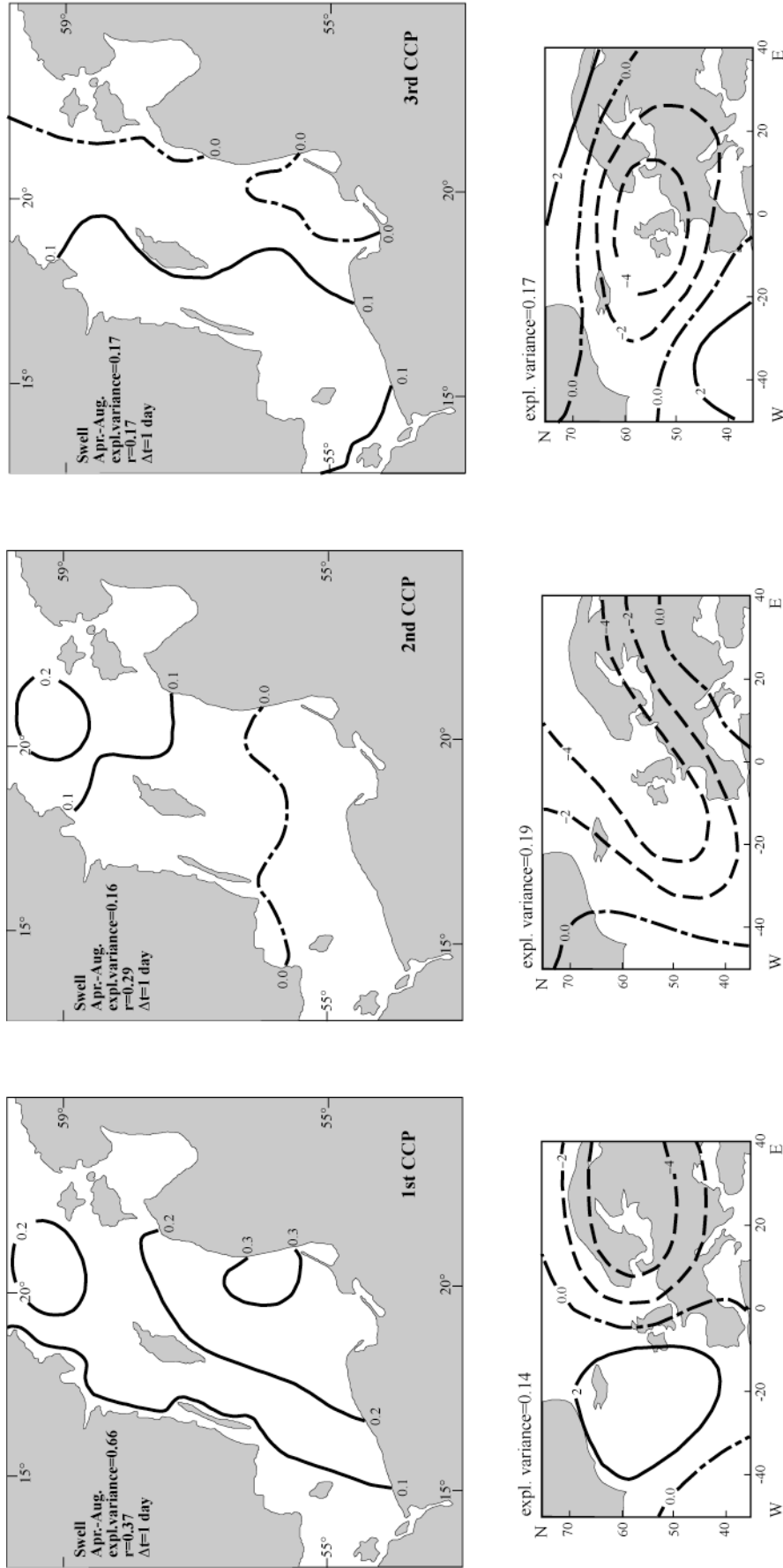
Fig. 10. The three first CCA pairs (from left to right) of air pressure anomalies (hPa) and swell height anomalies (m), for the "calm" season.

29
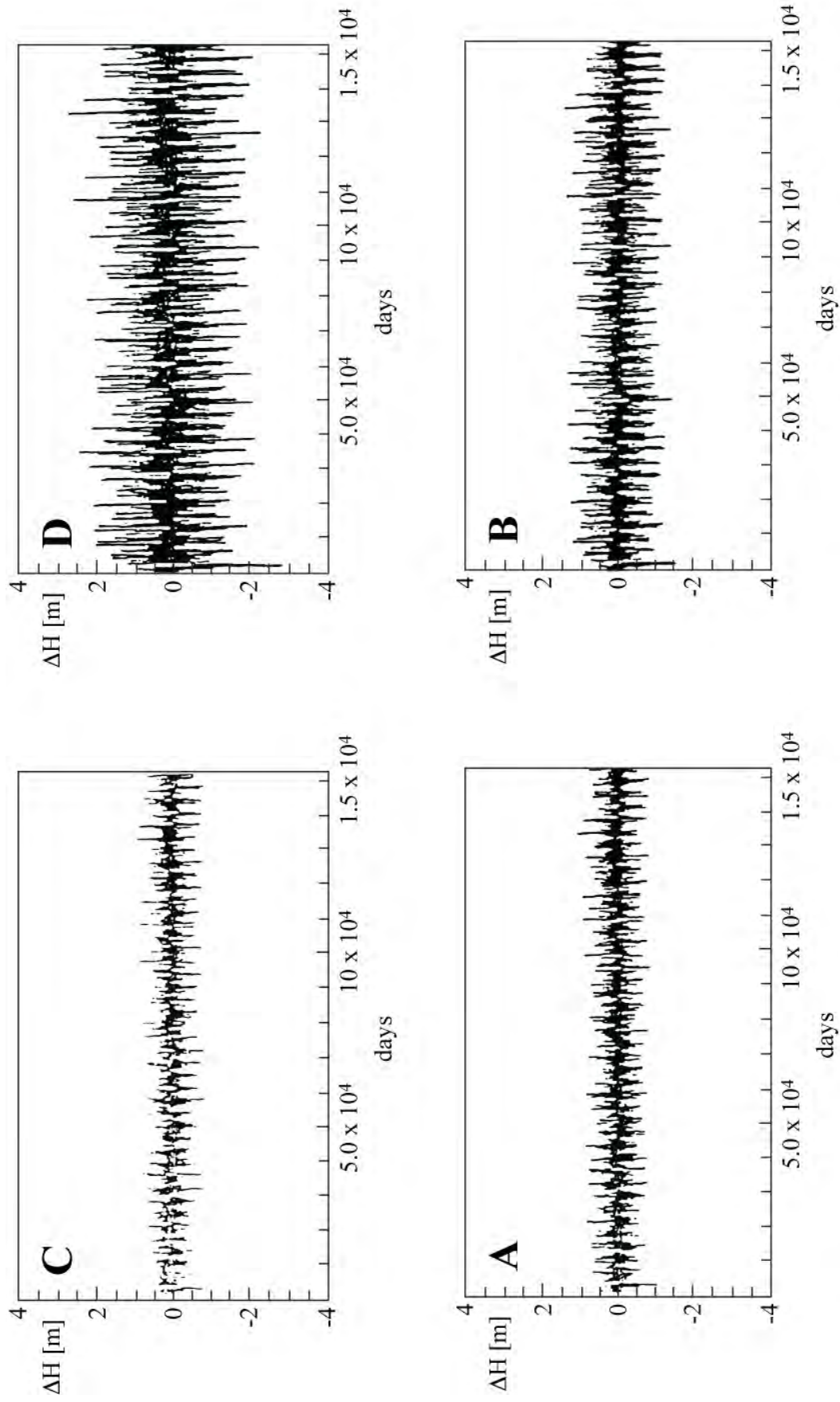
Fig. 11. The reconstructed time series of the total wave height at four selected points in the Proper Baltic Sea Basin, April 1947 - March 1988
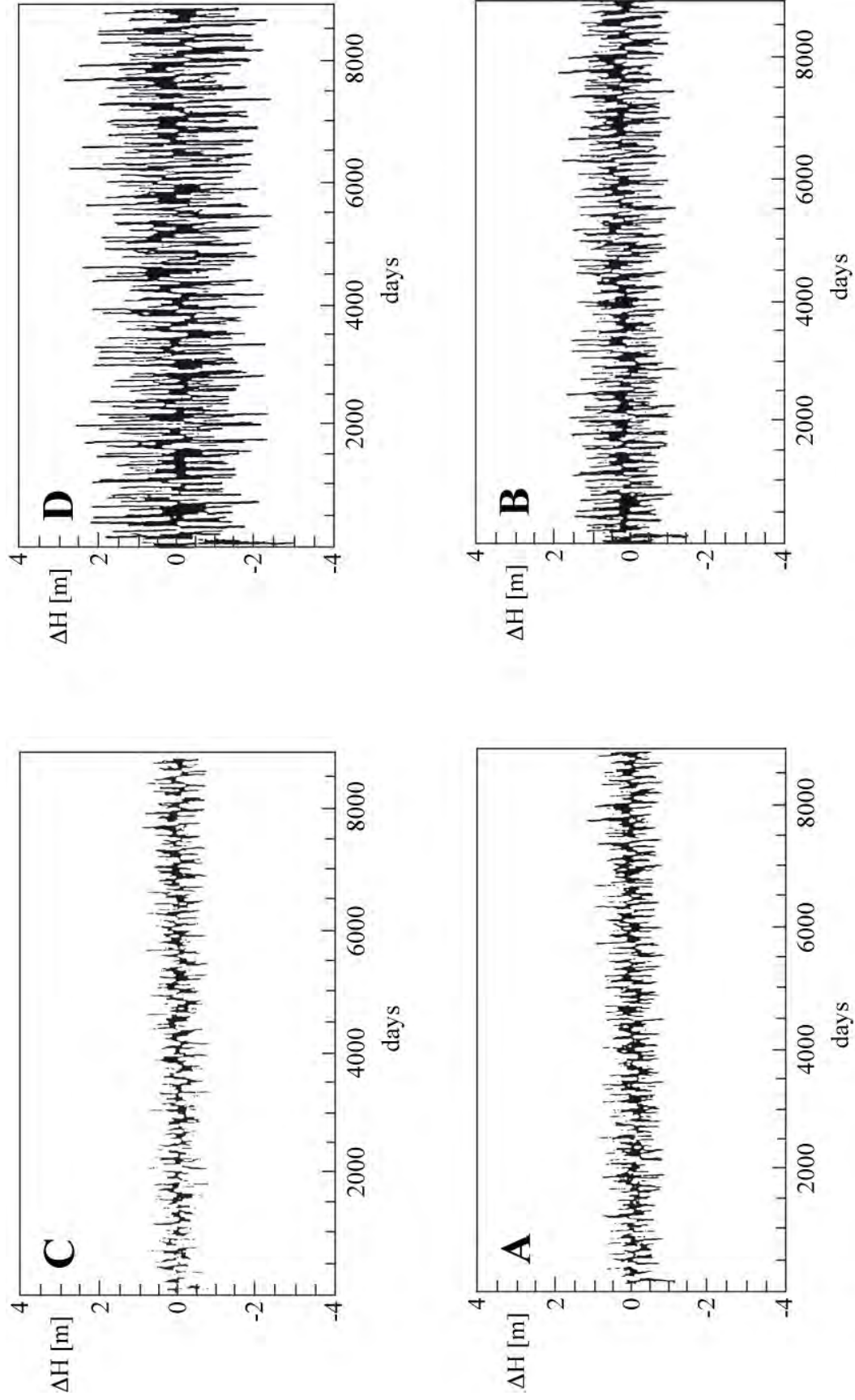
Fig. 12. The reconstructed time series of the total wave height for the "stormy" season at four selected points in the Proper Baltic Sea Basin, April 1947 - March 1988